Dual-Wavelength Soliton Mode-Locked Fiber Laser With a WS_2-Based Fiber Taper

Bo Guo, Yong Yao, Pei-Guang Yan, Ke Xu, Jing-Jing Liu, Shu-Guang Wang, and Yuan Li

***Abstract*— Recently, few-layer WS_2, as a novel two-dimensional (2D) material, has been discovered to possess both the saturable absorption effect and the huge nonlinear refractive index. In experiment, by taking advantage of the unique optical properties of 2D WS_2, we fabricated a highly nonlinear photonic device using the pulsed laser beam to deposit the WS_2 film onto a fiber taper. With the WS_2-based fiber taper, we have demonstrated the single- and dual-wavelength soliton pulses in the erbium-doped fiber laser (EDFL) by properly adjusting the pump strength and the polarization state. According to the soliton theory, the pulse width is ∼220 fs for the single-wavelength soliton, and ∼585 and ∼605 fs for the dual-wavelength soliton, respectively. The dual-wavelength soliton fiber laser exhibits the maximum output power of 10.1 mW and the pulse energy of ∼1.14 nJ, when the pump power is increased to ∼420 mW. Our findings suggest that WS_2-based fiber taper could operate as both an excellent saturable absorber for obtaining a femtosecond pulse and a promising highly nonlinear photonic material for the multi-wavelength generation.**

***Index Terms*— Mode-locked lasers, nonlinear optics, fibers, nonlinear optical materials, WS_2.**

I. Introduction

MULTI-WAVELENGTH mode-locked fiber lasers are of particular importance due to their versatile applications in optical communication, biomedical research and radar system [1]. So far, several actively/passively mode-locked techniques have been exploited for obtaining multi-wavelength soliton pulse in fiber lasers. Compared with active schemes, passive schemes share more benefits, such as very simple, compact and low-cost without a modulator required; easily achieve soliton pulse with ultrahigh peak power, and so on. To date, several passive mode-locking schemes have been used to generate multi-wavelength soliton pulse in the fiber lasers, such as nonlinear polarization rotation [2] and real saturable absorbers (SAs) (e.g., carbon nanotubes [3], graphene [4], and topological insulators (TIs) [5], [6]), and so on.

The discovery of graphene has triggered a worldwide upsurge in research interest in other 2D nanomaterials. Recently, a novel kind of layered material: transition metal dichalcogenides(TMDs), has gained great scientific and technical attention in physics, chemistry and material fields, owing to its high potential in electronic and optoelectronic applications [7]. TMDs can be expressed with the formula MX_2 (M = Mo, W, Ta, V, Nb, Re, Ti, etc; X=S, Se, Te). Due to specific 2D confinement of electron motion and an absence of interlayer coupling, monolayer TMD possesses a direct bandgap, making its nonlinear optical performance dramatically better than that of its bulk counterpart [8]. Since 2013, MoS_2, one kind of TMDs, has been found to be an efficient SA for mode-locked [8]–[13] or Q-switched [14], [15] fiber lasers at different wavelengths of 1064, 1550, and 1935 nm due to its excellent wideband saturable absorption behavior. Notably, WS_2, another layered TMD, has been exploited in electric field, such as catalysis, field-effect transistor, and so on [16]. However, its applicability in optics and optoelectronics is not fully studied. Quiet recently, few-layer WS_2 has been found to be another novel SAs for passively mode-locked [17]–[21] or Q-switched [22] fiber lasers. Several methods have been used to obtain the WS_2 SAs, such as optical deposition [18], pulsed laser deposition (PLD) [19], photonic crystal fiber (PCF) filling [20], side polished fiber or microfiber-based evanescent-field interaction [18], [21], and polymer film [22]. In these methods, the fiber ferrule-type SAs are simple and low-cost but have inherently short nonlinear interaction length [18]; PCF-filled SAs show the strong light-matter interaction but exhibit relatively larger insertion loss and distorted guiding mode in the PCF region [20]; the microfiber or side polished fiber-based SAs are attractive for high power tolerance and long interaction length, but not easy to obtain uniform material profile [21]; the 2D material polymer films could maintain the thermal stability of SAs, but they are vulnerable to destruction by high power operation [22].

Interestingly, PLD method is a well-known thin film fabrication technique but not fully exploited in 2D materials [19]. Compared with several preparation methods of WS_2-based SAs, PLD shows more benefits, such as good security component, high deposition rate and very uniform film. In addition, besides the saturable absorption behavior, Wang *et al.* also revealed that the 2D WS_2 itself shows a giant third order optical nonlinear refractive with a value of 10^{-11}m^2/W [23], which is similar with graphene [24], but much larger than TI: Bi_2Se_3 [24] and carbon nanotubes [25] (10^{-14} m^2/W^{-1}). Thus, if WS_2 film was deposited onto a fiber taper, it will exhibit the strong nonlinear optical response in 2D WS_2 and the sufficiently-long-range interaction length in fiber taper, making it could serve as both high nonlinear photonic device

Manuscript received August 3, 2015; revised October 17, 2015; accepted October 24, 2015. Date of publication October 27, 2015; date of current version December 22, 2015. This work was supported in part by the Guangdong Province Shenzhen Municipal Science and Technology Plan under Grant JC201105160592A and Grant 2010B090400306, in part by the Shenzhen Key Laboratory of Optical and Terahertz Meta-RF under Grant CXB201109210101A, and in part by the National Natural Science Foundation of China under Grant 61505039 and Grant 61575051.

B. Guo, Y. Yao, K. Xu, and Y. Li are with the School of Electronic and Information Engineering, Shenzhen Graduate School, Harbin Institute of Technology, Shenzhen 518055, China (e-mail: guobo512@163.com; yaoyong@hit.edu.cn; kxu@hitsz.edu.cn; liyuan13_a@126.com).

P.-G. Yan is with the Shenzhen Key Laboratory of Laser Engineering, College of Optoelectronic Engineering, Shenzhen University, Shenzhen 518060, China (e-mail: yanpg@szu.edu.cn).

J.-J. Liu is with Fujian Agriculture and Forestry University, Fuzhou 350002, China (e-mail: liu_jingjing@hotmail.com).

S.-G. Wang is with the School of Materials Science and Engineering, Shenzhen Graduate School, Harbin Institute of Technology, Shenzhen 518055, China (e-mail: wangshug2011@163.com).

Color versions of one or more of the figures in this letter are available online at http://ieeexplore.ieee.org.

Digital Object Identifier 10.1109/LPT.2015.2495330

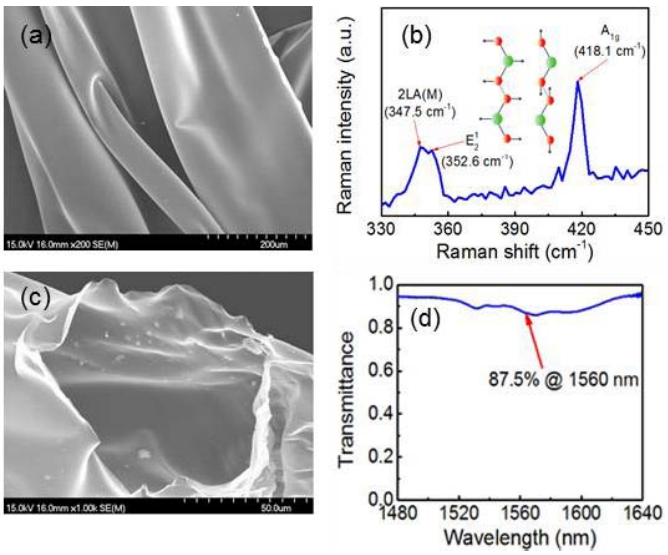

Fig. 1. Typical characteristics of the 2D WS_2 film: (a) and (c) show the SEM image of sample with the resolution of 200 μm and 50μm, respectively; (b) the Raman spectrum of WS_2 film; (d) the linear absorption spectrum of WS_2 film.

and SA in the laser cavity, which benefits for generating multi-wavelength mode-locked pulses [4]–[6] but not presented yet, to the best of our knowledge.

Here, we demonstrated the generation of single-, and dual-wavelength femtosecond soliton in an EDFL incorporating a WS_2-based fiber taper. The high-nonlinear photonic device could be used as both an excellent SA for mode-locking and a high-nonlinear medium for mitigating the mode competition of EDF and stabilizing the dual-wavelength oscillation. The WS_2-based fiber taper is prepared by the PLD method. The obtained results indicate that the WS_2 photonic device could be indeed a good candidate of highly-nonlinear photonic device for potential application fields, such as ultrafast nonlinear optics, biomedical research and radar system.

II. Preparation, Characterization and Optical Properties of WS_2-Based Fiber Taper

The as-used fiber-taper with waist diameter (~22 μm) and waist length (~1mm) were prepared by using the method similar to the previous reports [4], [19]. Next, we placed WS_2 target and fiber taper into a vacuum chamber where the vacuum degree was set at 5×10^{-4} pa. Then, a high-energy Nd:YAG laser with pulse energy of 2 mJ was focused on the WS_2 target to inspire the WS_2 plasma plume. Clearly, it would gradually grow on the surface of fiber taper to form the 2D film. In experiment, the thickness and length of WS_2 film could be roughly adjusted by controlling the pump strength and deposition time. Herein, the deposition time was ~1.5 hours.

To characterize the optical performance of the 2D WS_2 film, we fabricated it on a sheet of quartz glass under the same PLD process. Firstly, we characterized its morphological properties with an Auriga Cross-Beam Workstation (Carl Zeiss) scanning electron microscopy (SEM), as shown in Fig. 1(a) and Fig. 1(c), which reveal that the 2D WS_2 film exhibits sheet-like structure with wide distribution. Its average thickness is ~25 nm, which corresponds to ~80 layers, because the single-layer thickness of WS_2 is 0.315 nm [7]. Next, we characterized the crystalline structure of 2D WS_2 film with a Raman system (Renishaw Inc., New Mills, UK) using the 514 nm excitation line at room temperature. Clearly, two typical Raman peaks of WS_2 film centered at ~352.6 cm^{-1}, and ~418.1 cm^{-1}, as shown in Fig.1 (b), correspond to out-of-plane vibrational mode A_{1g} and in-plane vibrational mode E^1_{2g} of S-W-S lattice vibration, respectively.

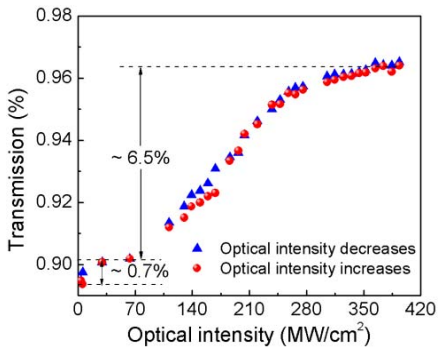

Fig. 2. The nonlinear saturable absorption curve of the WS_2-based fiber taper: the blue color and red color represents optical intensity of pump laser decreasing and increasing, respectively.

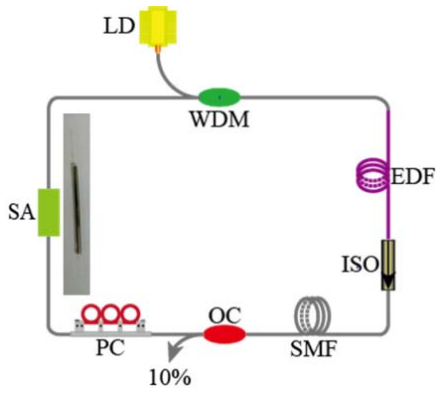

Fig. 3. Experimental setup, Inset: the photograph of the WS_2-based fiber taper.

To construct a practical WS_2 SA device, the WS_2 film on fiber-taper should be packaged, as shown in the inset of Fig. 3. Its linear transmission is ~87.5%@ 1560 nm, as shown in Fig. 1(d). Similar to the previous work [19], we obtain the WS_2 SA parameters, such as saturation intensity and modulation depth of ~20 MW/cm^2, ~0.7% (first saturable region), and ~370 MW/cm^2, ~6.5% (second saturable region) at 1550 nm, respectively, as depicted in Fig. 2, which measured with the power-dependent transmission technique. The as-used pump source is a femtosecond laser with pulse width of 500 fs and average power of 8 mW. In addition, the total insertion loss of the WS_2 SA is ~2.5 dB, which measured with a power meter.

III. Experimental Setup

The experimental setup of our proposed mode-locked fiber laser is shown in Fig. 3. The laser cavity consists of a piece of ~4.5 m highly doped Erbium-doped fiber (OFS, EDF) with dispersion parameter of ~−16.3 ps/(km · nm) and peak absorption of 14.5 dB/m at 1530 nm, and ~18.5 m single mode fiber (SMF) with dispersion parameter of 18 ps/(km · nm). The total net cavity dispersion is ~−0.36 ps^2. A fiber-pigtailed 980 nm laser diode (LD) via a fused 980/1550 wavelength-division multiplexer (WDM) is used to pump

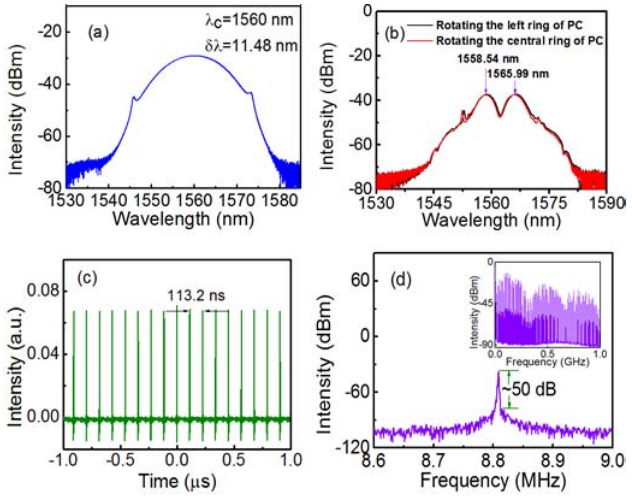

Fig. 4. Typical optical characteristics of the soliton pulses in the proposed fiber laser: (a) and (b) the optical spectrum of the single-wavelength soliton and dual-wavelength soliton pulse, respectively; (c) the pulse train, and (d) the corresponding RF spectrum of the dual-wavelength soliton pulse (Inset: broadband RF spectrum with 1GHz).

source, and a 10:90 optical coupler (OC) is employed to extract the output of the pulse. A polarization independent isolator (ISO) and a polarization controller (PC) are used to achieve unidirectional operation of the light in the ring cavity and adjust the polarization state of the propagation light, respectively. The optical performance of the pulse is measured by an optical spectrum analyzer (YOKOGAWA, AQ-6370C) with spectral resolution of 0.01 nm, a photo-detector (Thorlabs PDA, 10 GHz) combined with a 1 GHz mixed oscilloscope (Tektronix MDO4054-6, 5 GHz/s) and a power meter, respectively.

IV. Results and Discussions

Firstly, the fiber laser operates at continuous wave and appears into self-started traditional soliton mode-locking with the pump power of ~15 mW and ~40 mW, respectively, by properly adjusting the polarization state in the cavity. A series of experiments show that the stable single-, and dual-wavelength soliton can be easily obtained.

Next, we focus our discussion on the optical performance of the single-, and dual-wavelength soliton pulse when the pump power is ~80mW. By properly adjusting the PC, the typical single-wavelength soliton pulse is obtained, as shown in the Fig. 4(a). Clearly, its optical spectrum shows symmetrical Kelly sideband, implying that the optical pulse operates in the soliton mode-locking state. Its central wavelength is 1560 nm with 3-dB bandwidth of ~11.48 nm. Due to lack of proper autocorrelator, we can't measure its real duration time in experiment. However, we can estimate its theoretical limit of ~220 fs according to the soliton theory. Furthermore, by properly adjusting one (left or central) ring of the PC, the dual-wavelength soliton pulse is achieved equally, as shown in the Fig. 4(b). Their central wavelength is 1558.54 nm and 1565.99 nm with 3-dB bandwidth of ~4.2 nm and ~4.4 nm respectively. This implies that there are two separate pulse trains generated in dual-wavelength operation, each pulse with different duration of ~605fs and ~585fs, respectively. Meanwhile, it is seen from Fig. 4(c) that the pulse train has a period of 113.2 ns, corresponding to the fundamental cavity frequency ~8.83 MHz which matches with the cavity

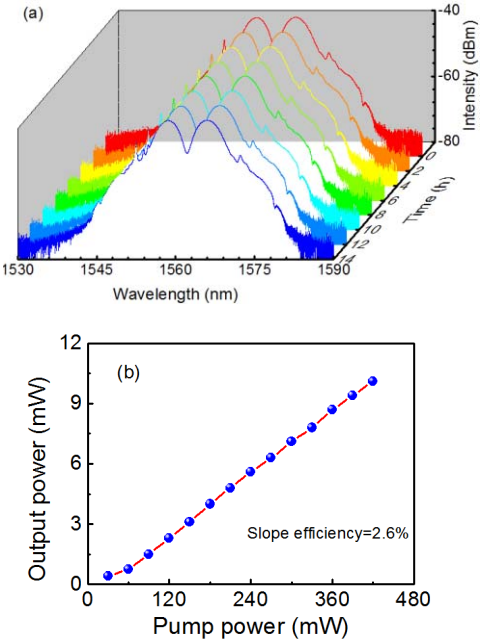

Fig. 5. (a) Long-term stability: optical spectra measured at a 2 hour-interval over 14 hours; (b) the output power versus the pump power of the dual-wavelength soliton pulse.

roundtrip time, thus verifies the mode-locking operation of the fiber laser.

To investigate the stability of the dual-wavelength soliton pulse, we provide its RF spectrum, as shown in Fig. 4(d). Its fundamental peak, located at the cavity repetition rate of 8.83 MHz, has a signal-to-noise ratio up to ~50 dB at a 500-Hz resolution bandwidth, indicating its good stability. Notably, we didn't observe two RF peaks in experiment. That's because, the separation between the two peaks of the RF spectrum is too small (~1.5 Hz) to distinguish clearly, according to the theoretical formula between the RF separation Δf and wavelength difference $d\lambda$ of the dual-wavelength soliton pulse as follows [2].

$$\Delta f = \frac{c^2 D d\lambda}{n^2(L + LDd\lambda c/n)} \tag{1}$$

Where D and L represents the dispersion parameter and the cavity length, respectively. c, and n is the light speed in vacuum and the refractive index of the fiber, respectively.

Furthermore, we also provide its RF spectrum in a wider range (1GHz), as shown in the inset of Fig. 4(d), the dual-wavelength soliton exhibits relatively good long-term stability. Notably, similar to our previous work [6], we can see that small modulation is presented due to the interaction between two soliton pulses. In addition, we can also examine the stability of the dual-wavelength soliton pulse by continuously monitoring its output spectra at a 2-hour interval over 14 hours, as shown in Fig. 5(a), which further indicates its long-term stability. Fig. 5(b) shows the average output power of the fiber laser as a function of pump power. It reveals a linear dependence of the output power of the laser on pump power and its slope efficiency is ~2.6%. Clearly, we find that the dual-wavelength soliton mode-locking operation is achieved above a threshold of 60 mW. Meanwhile, the maximum output power of 10.1 mW with the pulse energy of ~1.14nJ, peak power of ~1.95 kW and ~1.88 kW for the dual-wavelength soliton is obtained when pump power is ~420 mW.

To understand why the dual-wavelength soliton pulse could be formed in our laser, we notice that WS_2-based fiber taper exhibits huge third-order nonlinear effect, which originated from the evanescent field effect of taper structure [4], [10] and 2D WS_2 itself [23]. Thus, it is naturally to generate dual-wavelength soliton pulse in our proposed laser cavity due to the combination of the high nonlinear effect of the WS_2-based fiber taper and the spectral filtering effect. The latter is caused by the combination of the intra-cavity birefringence of SMF with polarization-dependent loss of PC [6]. In addition, to verify whether the dual-wavelength soliton pulse comes from the WS_2 SA, we tested the operation characteristic of the fiber laser without incorporating it in the cavity. By adjusting the pump strength and the cavity polarization state in a wide range, there is neither mode-locking nor dual-wavelength generation which excludes the possibility of nonlinear polarization evolution and Fabry-Perot cavity effect. Thus, the generation of dual-wavelength soliton pulse should originate from the WS_2 SA. In fact, similar to the previous work [5], we can obtain two separate wavelengths by using a band-pass filter to resolve the dual-wavelength soliton at each wavelength in future work.

Finally, it should be noticed that the saturable absorption of WS_2 SA near 1550 nm belongs to sub-bandgap absorption because the direct bandgap of monolayer WS_2 is $\sim$2.0 eV($\sim$630 nm) [17], the reason can be attributed to the defect [9], two-photon absorption [12], and absorption of edge mode [15], [22]. In experiment, PLD can produce very compete film and thus the absorption of defects should be weak; however, it is very difficult to obtain WS_2 with uniform shape and size. Therefore, there can be many edges in the WS_2-based photonic device leading to a relatively high absorption near 1550 nm. Although two-photon absorption may cause reverse saturable absorption, the saturable absorption of the WS_2 SA may still happen because the absorption of edge modes may play a bigger role in the cavity. Further investigation on the SA of 2D WS_2 is still required in future work.

V. Conclusion

In conclusion, we have achieved the single-, and dual-wavelength soliton pulse in an EDFL incorporating a WS_2-based fiber taper by properly adjusting the pump strength and polarization state. The WS_2-based fiber taper could be used as both an excellent SA for mode-locking and a high-nonlinear medium for mitigating the mode competition of EDF and stabilizing the dual-wavelength oscillation. The WS_2-based photonic device is prepared by using the PLD method. According to the soliton theory, the pulse width is $\sim$220 fs for the single-wavelength soliton; $\sim$585 fs and $\sim$605 fs for the dual-wavelength soliton, respectively. The dual-wavelength soliton fiber laser exhibits the maximum output power of 10.1 mW and pulse energy of $\sim$1.14 nJ at the pump power of $\sim$ 420 mW. Our study demonstrates that WS_2-based fiber taper can be operated as both a promising SA for ultrafast pulse generation and an excellent highly-nonlinear photonic material for many nonlinear optoelectronic applications.

References

[1] S. Li and K. T. Chan, "Electrical wavelength tunable and multiwavelength actively mode-locked fiber ring laser," *Appl. Phys. Lett.*, vol. 72, no. 16, pp. 1954–1956, Apr. 1998.

[2] D. Mao and H. Lu, "Formation and evolution of passively mode-locked fiber soliton lasers operating in a dual-wavelength regime," *J. Opt. Soc. Amer. B*, vol. 29, no. 10, pp. 2819–2826, Oct. 2012.

[3] Z. X. Zhang, Z. W. Xu, and L. Zhang, "Tunable and switchable dual-wavelength dissipative soliton generation in an all-normal-dispersion Yb-doped fiber laser with birefringence fiber filter," *Opt. Exp.*, vol. 20, no. 24, pp. 26736–26742, Nov. 2012.

[4] Z. Q. Luo, J. Z. Wang, M. Zhou, H. Y. Xu, Z. P. Cai, and C. C. Ye, "Multiwavelength mode-locked erbium-doped fiber laser based on the interaction of graphene and fiber-taper evanescent field," *Laser Phys. Lett.*, vol. 9, no. 3, pp. 229–233, Jan. 2012.

[5] M. Liu *et al.*, "Dual-wavelength harmonically mode-locked fiber laser with topological insulator saturable absorber," *IEEE Photon. Technol. Lett.*, vol. 26, no. 10, pp. 983–986, May 15, 2014.

[6] B. Guo, Y. Yao, J.-J. Xiao, R.-L. Wang, and J.-Y. Zhang, "Topological insulator-assisted dual-wavelength fiber laser delivering versatile pulse patterns," *IEEE J. Sel. Topics Quantum Electron.*, vol. 22, no. 2, Mar./Apr. 2016, Art. ID 0900108.

[7] Q. H. Wang, K. Kalantar-Zadeh, A. Kis, J. N. Coleman, and M. S. Strano, "Electronics and optoelectronics of two-dimensional transition metal dichalcogenides," *Nature Nanotechnol.*, vol. 7, pp. 699–712, Nov. 2012.

[8] H. Zhang *et al.*, "Molybdenum disulfide (MoS_2) as a broadband saturable absorber for ultra-fast photonics," *Opt. Exp.*, vol. 22, no. 6, pp. 7249–7260, Mar. 2014.

[9] S. Wang *et al.*, "Broadband few-layer MoS_2 saturable absorbers," *Adv. Mater.*, vol. 26, no. 21, pp. 3538–3544, Jun. 2014.

[10] H. Liu *et al.*, "Femtosecond pulse erbium-doped fiber laser by a few-layer MoS_2 saturable absorber," *Opt. Lett.*, vol. 39, no. 15, pp. 4591–4594, Aug. 2014.

[11] H. Xia *et al.*, "Ultrafast erbium-doped fiber laser mode-locked by a CVD-grown molybdenum disulfide (MoS_2) saturable absorber," *Opt. Exp.*, vol. 22, no. 14, pp. 17341–17348, Jul. 2014.

[12] R. Khazaeizhad, S. H. Kassani, H. Jeong, D. I. Yeom, and K. Oh, "Mode-locking of Er-doped fiber laser using a multilayer MoS_2 thin film as a saturable absorber in both anomalous and normal dispersion regimes," *Opt. Exp.*, vol. 22, no. 19, pp. 23732–23742, 2014.

[13] Z. Tian *et al.*, "Mode-locked thulium fiber laser with MoS_2," *Laser Phys. Lett.*, vol. 12, no. 6, p. 065104, Apr. 2015.

[14] Z. Luo *et al.*, "1-, 1.5-, and 2-μm fiber lasers Q-switched by a broadband few-layer MoS_2 saturable absorber," *J. Lightw. Technol.*, vol. 32, no. 24, pp. 4679–4686, Dec. 15, 2014.

[15] R. I. Woodward *et al.*, "Tunable Q-switched fiber laser based on saturable edge-state absorption in few-layer molybdenum disulfide (MoS_2)," *Opt. Exp.*, vol. 22, no. 25, pp. 31113–31122, Dec. 2014.

[16] T. Georgiou *et al.*, "Vertical field-effect transistor based on graphene–WS_2 heterostructures for flexible and transparent electronics," *Nature Nanotechnol.*, vol. 8, pp. 100–103, Dec. 2012.

[17] X. Fu, J. Qian, X. Qiao, P. Tan, and Z. Peng, "Nonlinear saturable absorption of vertically stood WS_2 nanoplates," *Opt. Lett.*, vol. 39, no. 22, pp. 6450–6453, 2014.

[18] D. Mao *et al.*, "WS_2 mode-locked ultrafast fiber laser," *Sci. Rep.*, vol. 5, Jan. 2015, Art. ID 7965.

[19] P. Yan *et al.*, "Microfiber-based WS_2-film saturable absorber for ultra-fast photonics," *Opt. Mater. Exp.*, vol. 5, no. 3, pp. 479–489, Feb. 2015.

[20] P. Yan *et al.*, "Passively mode-locked fiber laser by a cell-type WS_2 nanosheets saturable absorber," *Sci. Rep.*, vol. 5, Jul. 2015, Art. ID 12587.

[21] R. Khazaeinezhad *et al.*, "Ultrafast pulsed all-fiber laser based on tapered fiber enclosed by few-layer WS_2 nanosheets," *IEEE Photon. Technol. Lett.*, vol. 27, no. 15, pp. 1581–1584, Aug. 1, 2014.

[22] K. Wu, X. Zhang, J. Wang, X. Li, and J. Chen, "WS_2 as a saturable absorber for ultrafast photonic applications of mode-locked and Q-switched lasers," *Opt. Exp.*, vol. 23, no. 9, pp. 11453–11461, Apr. 2015.

[23] G. Wang *et al.*, "Tunable nonlinear refractive index of two-dimensional MoS_2, WS_2, and $MoSe_2$ nanosheet dispersions [invited]," *Photon. Res.*, vol. 3, no. 2, pp. A51–A55, 2015.

[24] S. Lu *et al.*, "Third order nonlinear optical property of Bi_2Se_3," *Opt. Exp.*, vol. 21, no. 2, pp. 2072–2082, Jan. 2013.

[25] N. Kamaraju, S. Kumar, A. K. Sood, S. Guha, S. Krishnamurthy, and C. N. R. Rao, "Large nonlinear absorption and refraction coefficients of carbon nanotubes estimated from femtosecond z-scan measurements," *Appl. Phys. Lett.*, vol. 91, no. 25, p. 251103, Mar. 2007.